IEEE Photonics Journal
An IEEE Photonics Society Publication

Open Access

Identification of Malaria-Infected Red Blood Cells Via Digital Shearing Interferometry and Statistical Inference

Volume 5, Number 5, October 2013

I. Moon, Member, IEEE
A. Anand
M. Cruz
B. Javidi, Fellow, IEEE

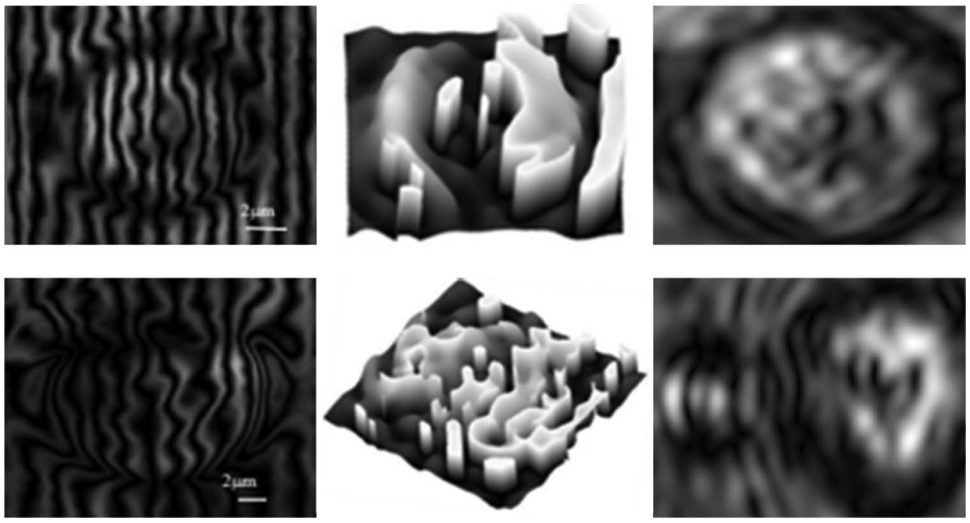

DOI: 10.1109/JPHOT.2013.2278522
1943-0655

IEEE photonics SOCIETY

IEEE

Identification of Malaria-Infected Red Blood Cells Via Digital Shearing Interferometry and Statistical Inference

I. Moon,[1] ***Member, IEEE*****, A. Anand,**[2] **M. Cruz,**[3] **and B. Javidi,**[4] ***Fellow, IEEE***

[1]School of Computer Engineering, Chosun University, Gwangju 501-759, Korea
[2]Department of Applied Physics, Faculty of Technology and Engineering, The MS University of Baroda, Vadodara-390 001, India
[3]Universidad Autónoma del Carmen, 24180, Ciudad del Carmen, Campeche, Mexico
[4]Department of Electrical and Computer Engineering, University of Connecticut, Storrs, CT 06269-2157 USA

DOI: 10.1109/JPHOT.2013.2278522

Manuscript received August 2, 2013; accepted August 2, 2013. Date of publication August 15, 2013; date of current version August 30, 2013. This work was supported in part by CONACyT, Mexico, and in part by scholarship 162914. The work of I. Moon was supported by the Basic Science Research Program through the National Research Foundation of Korea (NRF) funded by the Ministry of Education, Science and Technology under Grant NRF-2013R1A2A2A05005687. The work of A. Anand was supported in part by research funding through DST-FIST and UGC-DRS projects and in part by UGC under major research Grant 42-776/2013(SR). Corresponding author: I. Moon (e-mail: inkyu.moon@chosun.ac.kr).

Abstract: Malaria is one of the most widespread diseases, particularly in Asia and Africa. Correct diagnosis of malaria is necessary for its proper treatment. A compact automated tool for malaria identification will greatly benefit healthcare professionals in these regions. We propose a method that has the potential to automatically detect malaria-infected red blood cells (RBCs). This method combines the simplicity and robustness of lateral shearing interferometry with the flexibility of statistical methods to achieve the classification of diseased RBCs. Shearing interferograms generated using a glass plate in a common path setup were Fourier analyzed to retrieve the gradient phase and amplitude information of the cell. Then, multiple features based on the complex amplitude information of the cells are measured automatically and used to differentiate healthy and malaria-infected cells. Multivariate statistical inference algorithm of the experimental data shows that there is a difference between the populations of healthy and malaria-infected RBCs by using the measured RBC features.

Index Terms: Medical and biological imaging, interferometry, pattern recognition, microscopy.

1. Introduction

Malaria is widespread in Africa and Asia and is potentially fatal, which makes correct diagnosis crucial for proper treatment. Microscopic analysis of cells is an important process in the diagnosis of malaria [1]–[3]. However, it currently requires the use of chemical reagents, special equipment and qualified personnel, restricting its use in under developed and remote zones. In developing countries, microscopic inspection of blood smears by a qualified technician is still the gold standard in malaria diagnosis. Visual identification of malarial red blood cells (RBCs) may be unreliable if there is a lack of sufficiently trained technicians plus poor quality microscopes and reagents used for staining the blood smears. Non-invasive techniques based on interferometry [4]–[16], such as digital holographic microscopy [4]–[11] and optical coherence microscopy [12], [13], provide

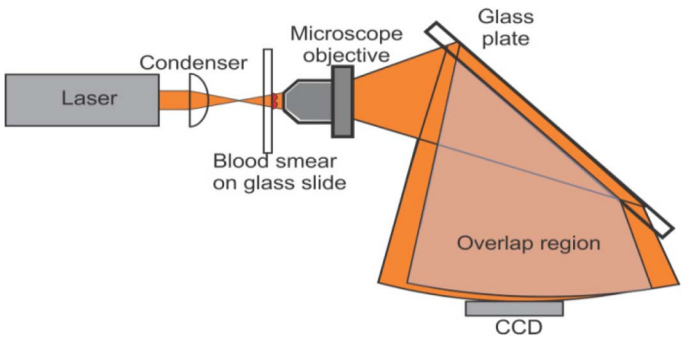

Fig. 1. Experimental setup for generating the shearing interferogram to measure the complex amplitude of RBCs.

complex field distributions and have proven to be a good option in the label free study of microorganisms for their identification and comparison.

In this paper, we propose the use of lateral shearing interferometry [17], [18] and statistical inference for RBC identification. Shearing interferometry is a technique mainly used in optical testing to measure aberrations in optical elements. Here, the object wavefront is split into two, and one beam is slightly displaced. This displacement can be lateral, radial or rotational. The original wavefront is retrieved using a set of differential equations or Zernike polynomials [19]. In the present technique, a shearing interferogram is generated with a spherical wavefront that illuminates the object and is then reflected by a glass plate onto an imaging sensor, making it a single path system. Fourier analysis of the interferograms yields the gradient phase and amplitude information of the cell. This information will be used for the RBC classification process.

We use sample statistics to estimate the RBC population parameters. The statistical sampling method allow us to make decisions about the two RBC populations (healthy and malaria infected RBCs) on the basis of sample information. The statistical sampling methods were already found to yield good results in the analysis and classification of cells where the cell data description is complex and variable [20], [21]. In our previous work, we used a Mach–Zehnder digital holographic microscope to record the digital hologram of the red blood cells [22]. Correlation algorithms were used on the shape information of the cells to distinguish between healthy and diseased red blood cells. Correlation algorithms while simple in implementation were not very effective in classifying the diseased red blood cells. Also, the Mach–Zehnder digital holographic microscope is more complex than the lateral shearing interferometry digital holographic microscope presented in this paper. In the proposed technique, we first extract features from healthy and malaria infected RBCs measured at single cell level using lateral shearing interferometry, and then apply Hotelling's T-square statistics [23], [24] to the sample units to infer whether the malaria infected RBCs are significantly different from healthy RBCs. The Hotelling's T-square tests in our experiments show that the measured features have the potential to differentiate between populations of healthy and malaria infected RBCs. It should be noted here that our main interest lies not in the retrieval of the object wavefront, but in the recovery of sufficient information for classification of the cells. Therefore, it can be possible to decide on the basis of sample data whether the proposed procedure is really effective in identifying the malaria infected RBCs.

2. Experimental Details and Results

A schematic of the experimental setup is shown in Fig. 1. A HeNe laser ($\lambda = 611.8$ nm, 2mW, random-linearly polarized) is used as the source. Alternatively, a cheap diode laser can also be used. The beam passes through a condenser lens (which was a 20X microscopic objective lens with NA $= 0.4$) and then through the object. A microscope objective (oil immersion, $100\times$, NA $= 1.25$) magnifies the object wavefront. Sample was kept at the working distance of the microscopic objective. Then, the beam is split using a thin glass slide of 0.1 mm thickness (which

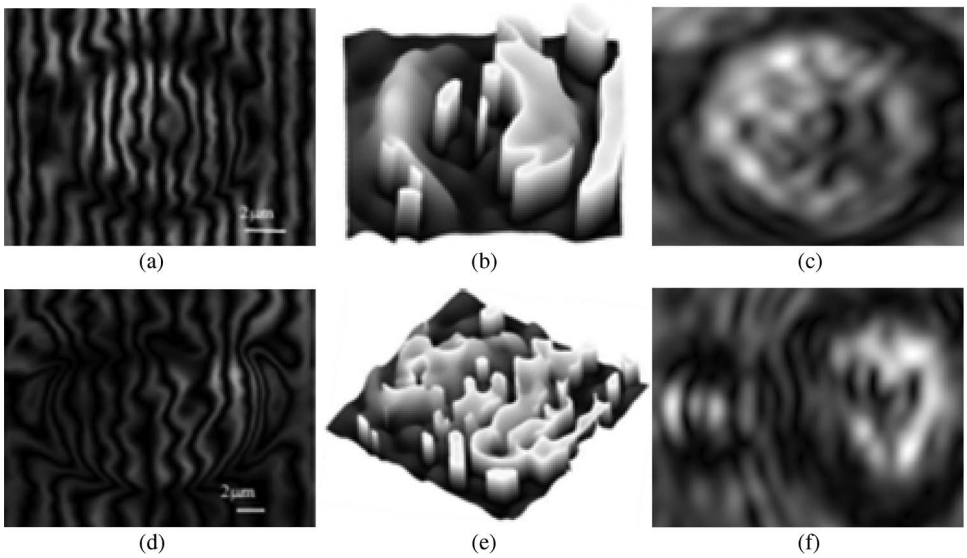

Fig. 2. (a), (d) Shearing interferograms. (b), (e) RBC gradient phase image retrieved from shearing interferograms in (a) and (d), respectively. (c), (f) RBC gradient amplitude image retrieved from shearing interferograms in (a) and (d) respectively. (a)–(c) Are from a healthy RBC, whereas (d)–(f) are from a malaria infected RBC.

acts as the shearing element) kept at 45° to the axis of the magnifying lens, which results in the wavefronts being laterally sheared at the detector plane (see Fig. 1). The shearing plate was kept a distance of 90 mm from the collar of the objective lens. The interferograms were recorded by a CCD (8-bit dynamic range, 1024 × 1024 pixels, 4.65 μm pixel pitch) placed at the image plane (160 mm from collar of the objective lens) of the magnifying lens. If the curvature of the spherical wavefront is low (almost plane) and the thickness of the shearing plate is small, we can assume that the wavefronts reflected from both faces of the glass plate have almost the same curvature, resulting in a linear fringe system. Healthy red blood cells were obtained after centrifugation of blood samples taken from individuals with no known diseases or illnesses. Blood samples were also collected from individuals detected with severe malaria. These samples were also centrifuged to separate malaria-infected RBCs. Thin blood smears of both sample were formed on glass slides. Shearing interference patterns of both healthy and malaria infected RBCs were then recorded (Fig. 2(a) and (d) respectively). These interference patterns were then Fourier analyzed to obtain the gradient phase and intensity information about the object wavefront.

If the object transmittance function is defined as $a_o(x,y)\exp[i\varphi_o(x,y)]$ and we assume that the illuminating beam is a spherical wave, the recorded interferogram can be written as:

$$\begin{aligned} I_o(x,y) = {} & |a_o(x,y)|^2 + |a_o(x+\Delta x,y)|^2 \\ & + |a_o(x,y)|\ |a_o(x+\Delta x,y)| \exp\{i[\varphi_o(x,y) - \varphi_o(x+\Delta x,y)] + ik2x\Delta x/z + ik\Delta x^2/z\} \\ & + |a_o(x,y)|\ |a_o(x+\Delta x,y)| \exp\{-i[\varphi_o(x,y) - \varphi_o(x+\Delta x,y)] - ik2x\Delta x/z - ik\Delta x^2/z\} \end{aligned} \tag{1}$$

where $k = 2\pi/\lambda$ and z is the curvature radius of the wavefront at the CCD plane. We then apply the Fourier Transform (FT) to Eq. (1). The spectrum of the first two terms is the zero order. The spectrum of the last two terms appears separated from the center by $\pm 4\pi x\Delta x/\lambda z$, due to the linear phase term with opposite sign. We filter one of these spectrums and apply the inverse FT. The retrieved field includes the phase difference between the original and sheared wavefront, the linear phase and a constant phase factor that depends on Δx^2. The last two phase terms are eliminated either by using an approximation or by subtracting the phase retrieved from a

reference interferogram recorded without an object. The resultant phase contains only the phase difference between the sheared wavefronts, i.e. the gradient phase. This field is used in the RBC classification process. It is also possible to use a plane wave as the illumination wave but then it is necessary to introduce a tilt in one of the wavefronts using a wedge plate instead of the parallel shearing plate [18].

The healthy RBCs have a smooth disc structure with a collapsed center and no nucleus. On the contrary, the cell structure of those infected by malaria parasites were found to deviate from the disc like structure depending on the severity of infection. When the malaria parasite infects a RBC, it enters the cell to hide itself from the body's defenses and begins to reproduce itself inside of the RBC until the cell is damaged. The phase of the illuminating beam is modified by the internal structure of the cell under investigation. If the cell is healthy, its phase will have a smooth shape. But if the cell is infected, the phase will have abrupt changes corresponding to the presence of the malaria parasites. We have used these disparities between healthy and diseased RBCs to classify the cells. The classifier compares the information of each cell against the information of a prototype of a healthy cell. If the information is sufficiently different, the cell is classified as a diseased cell.

In Fig. 2, the shearing interferograms and the gradient phase and amplitude images for healthy and malaria infected RBCs are shown. In order to investigate the difference of statistical parameters between the two RBC populations (healthy and malaria infected ones), six features are extracted from the selected area of each cell image obtained via digital shearing interferometry and then used for statistical hypothesis testing. The six properties are defined as: (1) average value of the gradient phase image; (2) average value of the gradient amplitude image; (3) average value of the amplitude image obtained by applying the Fourier transform to the gradient phase image; (4) D1-value i.e., the maximal value minus minimal value in the amplitude image obtained by applying the Fourier transform to the gradient phase image; (5) average value of the amplitude image obtained by applying the Fourier transform to the gradient amplitude image; (6) D2-value i.e., maximal value minus minimal value in the amplitude image obtained by applying the Fourier transform to the gradient amplitude image. The six features are expressed as variables from X_1 to X_6. The last four features are the analysis of the gradient phase and amplitude images in the frequency domain.

For statistically evaluating the difference of the two RBC populations in healthy (c1: class 1) and malaria infected (c2: class 2) cells, we assume that two random samples of sizes n_{c1} and n_{c2} are drawn from the corresponding six-variate normal populations $(N_{c1}(\mu_{c1}, S_{c1})$ or $N_{c2}(\mu_{c2}, S_{c2}))$ and have the same covariance. To test the hypothesis H_0 that the random samples come from the same population (i.e., $\mu_{c1} = \mu_{c2}$, as well as $S_{c1} = S_{c2}$), we use the following variable T^2 [24]:

$$T^2 = \frac{n_{c1} n_{c2}}{n_{c1} + n_{c2}} (\bar{y}_{c1} - \bar{y}_{c2})' S_{pl}^{-1} (\bar{y}_{c1} - \bar{y}_{c2}). \tag{2}$$

Eq. (2) satisfies the Hotelling's T-squared distribution as $T^2_{p,n_{c1}+n_{c2}-2}$ when $H_0 : N_{c1}(\mu_{c1}, S_{c1}) = N_{c2}(\mu_{c2}, S_{c2})$ is true, where n_{c1} and n_{c2} are the number of observations in class 1 and class 2, respectively. $\bar{y}_{c1}$ and $\bar{y}_{c2}$ are represented as follows [23]:

$$\bar{y}_{c1} = \sum_{i=1}^{n_{c1}} y_{1i}/n_{c1}, \qquad \bar{y}_{c2} = \sum_{i=1}^{n_{c2}} y_{2i}/n_{c2} \tag{3}$$

where y_{1i} and y_{2i} are random samples from the two specific populations while each sample has six features. The S_{pl} in Eq. (2) is the common population covariance matrix which is expressed as:

$$S_{pl} = \frac{1}{n_{c1} + n_{c2} - 2} \times \left[\sum_{i=1}^{n_{c1}} (y_{1i} - \bar{y}_{c1})(y_{1i} - \bar{y}_{c1})' + \sum_{i=1}^{n_{c2}} (y_{2i} - \bar{y}_{c2})(y_{2i} - \bar{y}_{c2})' \right] \tag{4}$$

where S_{pl}^{-1} is the inverse of S_{pl}.

Statistical hypothesis testing [T^2-test] was performed in order to analyze the equality between the population of healthy and malaria infected RBCs with the defined six variables, where both of the two random samples of sizes n_{c1} and n_{c2} were 5. The statistical p-value was calculated to be

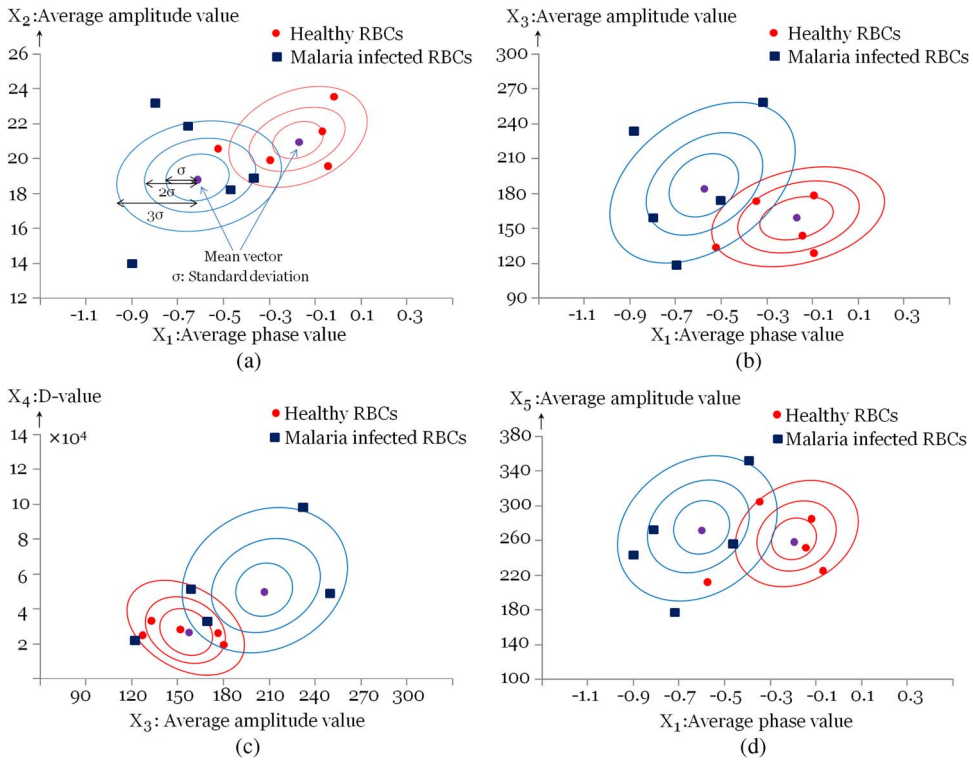

Fig. 3. Scatter plot for selected pairs (as defined in the text) of calculated features from the shearing interferograms in healthy and malaria infected RBCs. (a) Scatter plot for variables X_1 and X_2. (b) Scatter plot for variables X_1 and X_3. (c) Scatter plot for variables X_3 and X_4. (d) Scatter plot for variables X_1 and X_5.

0.00926 by employing F distribution in [23] after transforming the T^2-statistics into an F-statistics using the following equation [23]:

$$\frac{n_1 + n_2 - p - 1}{(n_1 + n_2 - 2)p} T^2 = F_{p,n_1+n_2-p-1} \tag{5}$$

where p is the number of variables $(=$ number of features$)$ and $n_1 + n_2 - p - 1$ is the first degree-of-freedom parameter for the F-statistics. The statistical p-value approximately reveals the probability that the observed test statistic in Eq. (2) would happen in the same population. Consequently, the obtained p-value (0.00926) in this experiment illustrates that the distinction between the two RBC populations are significant since we can reject the null hypothesis, $[H_0 : N_{c1}(\mu_{c1}, S_{c1}) = N_{c2}(\mu_{c2}, S_{c2})]$, at the 0.01 level of significance. In Fig. 3, the scattering plots for selected pairs of variables, which visually reveal the division of the healthy and malaria infected RBCs, are shown.

Moreover, in order to show that each feature would significantly increase the separation of the two sampling units (healthy and malaria infected RBCs), the test for additional information [24] is conducted. Here, the null hypothesis for this test is that a single variable is redundant for separating the two groups, that is, the extra variable do not contribute anything significant beyond information already available in the other variables for separating the groups. The test statistic for the significance of adding a single variable/feature x to the p variables/features denoted as vector $\mathbf{y}$ can be described as following equation [24] [For example, the test statistic for the significance of adding a variable $X_1(x = X_1)$ to the other five $(p = 5)$ variables $\mathbf{y} = (X_2, X_3, X_4, X_5, X_6)$ is expressed as:

$$T^2(x|\mathbf{y}) = (v - p)\frac{T^2_{p+1} - T^2_p}{v + T^2_p}. \tag{6}$$

$T^2(x|y)$ is distributed as $T^2_{1,v-p}$ where $v = n_{c1} + n_{c2} - 2$, while T^2_{p+1} and T^2_p are defined as Eq. (2). For checking the significance of each feature among total six features, six null hypothesis [(1) H_0: X_1 is redundant, (2) H_0: X_2 is redundant, (3) H_0: X_3 is redundant, (4) H_0: X_4 is redundant, (5) H_0: X_5 is redundant, (6) H_0: X_6 is redundant] are required and tested separately. The statistical p-values derived from the corresponding test statistic in Eq. (6) for the six null hypothesis are 0.00442, 0.00442, 0.00442, 0.00442, 0.00441, and 0.01149, respectively. It is noted that all of the six null hypothesis should be rejected and conclusion can be made that each variable makes a significant contribution to the separation of the two groups (healthy and malaria infected RBCs) at the 0.05 level of significance. Also, experimental results reveal that the first five features almost contribute the same importance to discriminate the malaria infected RBCs from others and provide more information than that of the last feature.

3. Conclusion

In this paper, we have presented a simple approach to identify malaria infected RBCs via lateral shearing interferometry and statistical sampling. The shearing interferograms were generated by using a glass plate in a single path setup. Fourier analysis of the interferogram was conducted to obtain the gradient complex amplitude information of the cell. For the purpose of recognition of malaria infected cells, six features were extracted from complex information obtained from each healthy and malaria infected cells. Then, statistical inference was performed to see if the multivariate random samples with six features come from the same population. It should be noted that the shear amount affects only the density of the fringes. But since the two images (from the front and back surface of the parallel plate) should overlap to form the shear interference pattern, the thickness of the plate was kept to a value which achieves this. Discrimination of the cells is obtained from the reconstructed gradient phase and intensity information, which was achieved using Fourier fringe analysis. So the discrimination probability does not depend upon the shear amount. We have experimentally demonstrated that the complex amplitude data captured by shearing interferometry has the potential to be used to classify healthy and malaria infected RBCs using statistical inference. The experimental setup being simple and compact makes it possible to construct a cheap, field portable version of the technique using laser diodes and CMOS sensors.

References

[1] D. Warhurts and J. Williams, "ACP broadsheet no. 148, laboratory diagnosis of malaria," *J. Clin. Pathol.*, vol. 49, no. 7, pp. 533–538, Jul. 1996.
[2] D. Cojoc, S. Finaurini, P. Livshits, E. Gur, A. Shapira, V. Mico, and Z. Zalevsky, "Toward fast malaria detection by secondary speckle sensing microscopy," *Biomed. Opt. Exp.*, vol. 3, no. 5, pp. 991–1005, May 2012.
[3] Y. Park, M. Diez-Silva, D. Fu, G. Popescu, W. Choi, I. Barman, S. Suresh, and M. Feld, "Static and dynamic light scattering of healthy and malaria-parasite invaded red blood," *J. Biomed. Opt.*, vol. 15, no. 2, p. 020506, Mar./Apr. 2010.
[4] P. Girshovitz and N. Shaked, "Generalized cell morphological parameters based on interferometric phase microscopy and their application to cell life cycle characterization," *Biomed. Opt. Exp.*, vol. 3, no. 8, pp. 1757–1773, Aug. 2012.
[5] P. Marquet, B. Rappaz, P. Magistretti, E. Cuche, Y. Emery, T. Colomb, and C. Depeursinge, "Digital holographic microscopy: A noninvasive contrast imaging technique allowing quantitative visualization of living cells with subwavelength axial accuracy," *Opt. Lett.*, vol. 30, no. 5, pp. 468–470, Mar. 2005.
[6] W. Xu, M. Jericho, I. Meinertzhagen, and H. Kreuzer, "Digital in-line holography for biological applications," *Proc. Nat. Acad. Sci.*, vol. 98, no. 20, pp. 11 301–11 305, Sep. 2001.
[7] P. Ferraro, D. Alferi, S. De Nicola, L. De Petrocellis, A. Finizio, and G. Pierattini, "Quantitative phase-contrast microscopy by a lateral shear approach to digital holographic image reconstruction," *Opt. Lett.*, vol. 31, no. 10, pp. 1405–1407, May 2006.
[8] T. Kreis, *Handbook of Holographic Interferometry: Optical and Digital Methods*. New York, NY, USA: Wiley-VCH, 2005.
[9] V. Micó, Z. Zalevsky, C. Ferreira, and J. García, "Superresolution digital holographic microscopy for three dimensional samples," *Opt. Exp.*, vol. 16, no. 23, pp. 19 260–19 270, Nov. 2008.
[10] C. Oh, S. Isikman, B. Khademhosseinieh, and A. Ozcan, "On-chip differential interference contrast microscopy using lensless digital holography," *Opt. Exp.*, vol. 18, no. 5, pp. 4717–4726, Mar. 2010.
[11] L. Miccio, A. Finizio, R. Puglisi, D. Balduzzi, A. Galli, and P. Ferraro, "Dynamic DIC by digital holography microscopy for enhancing phase-contrast visualization," *Opt. Exp.*, vol. 2, no. 2, pp. 331–344, Jan. 2011.

[12] P. Torok and F. Kao, *Optical Imaging and Microscopy: Techniques and Advanced Systems*. Berlin, Germany: Springer-Verlag, 2003.
[13] A. Bachmann, R. Michaely, T. Lasser, and R. Leitgeb, "Dual beam heterodyne Fourier domain optical coherence tomography," *Opt. Exp.*, vol. 15, no. 15, pp. 9254–9266, Jul. 2007.
[14] S. Nicola, P. Ferraro, A. Finizio, G. Pesce, and G. Pierattini, "Reflective grating interferometer for measuring the refractive index of transparent materials," *Opt. Commun.*, vol. 118, no. 5/6, pp. 491–494, Aug. 1995.
[15] M. Kim, Y. Choi, C. Yen, Y. Sung, K. Kim, R. Dasari, M. Feld, and W. Choi, "Three-dimensional differential interference contrast microscopy using synthetic aperture imaging," *J. Biomed. Opt.*, vol. 17, no. 2, p. 026003, Feb. 2012.
[16] G. Goppola, G. Di Caprio, M. Gioffré, R. Puglisi, D. Balduzzi, A. Galli, L. Miccio, M. Paturzo, S. Grilli, A. Finizio, and P. Ferraro, "Digital self-referencing quantitative phase microscopy by wavefront folding in holographic image reconstruction," *Opt. Lett.*, vol. 35, no. 20, pp. 3390–3392, Oct. 2010.
[17] A. Singh, A. Anand, R. Leitgeb, and B. Javidi, "Lateral-shearing digital holographic imaging of small biological specimens," *Opt. Exp.*, vol. 20, no. 21, pp. 23 617–23 622, Oct. 2012.
[18] G. Pedrini, Y. Zou, and H. Tiziani, "Quantitative evaluation of digital shearing interferogram using the spatial carrier method," *Pure Appl. Opt.*, vol. 5, no. 3, pp. 313–321, May 1996.
[19] D. Malacara, *Optical Shop Testing*. New York, NY, USA: Wiley, 1992.
[20] B. Javidi, I. Moon, S. K. Yeom, and E. Carapezza, "Three-dimensional imaging and recognition of microorganism using single-exposure on-line (SEOL) digital holography," *Opt. Exp.*, vol. 13, no. 12, pp. 4492–4506, Jun. 2005.
[21] I. Moon, M. Daneshpanah, A. Stern, and B. Javidi, "Automated three-dimensional identification and tracking of micro/nano biological organisms by computational holographic microscopy," *Proc. IEEE*, vol. 97, no. 6, pp. 990–1010, Jun. 2009.
[22] A. Anand, V. K. Chhaniwal, N. R. Patel, and B. Javidi, "Automatic identification of malaria-infected RBC with digital holographic microscopy using correlation algorithms," *IEEE Photon. J.*, vol. 4, no. 5, pp. 1456–1464, Oct. 2012.
[23] R. Bartoszynski and M. Niewiadomska-Bugaj, *Probability and Statistical Inference*. New York, NY, USA: Wiley-Interscience, 2007.
[24] A. Rencher, *Methods of Multivariate Analysis*. New York, NY, USA: Wiley-Interscience, 2002.